Modelling hydration effect on the mechanical performance of polyamide 6.6/glass fibers composites

Allan Oliveira Rodrigues[1] [iD], Gabriel Fornazaro[1]* [iD], Gabriel Vinicius Alves Silva[1] [iD], Eduardo Radovanovic[2] [iD], Andressa dos Santos[1] [iD], Hederson Majela do Nascimento[1] [iD], Antonio Guilherme Basso Pereira[3] [iD] and Silvia Luciana Favaro[1] [iD]

[1]Laboratório de Engenharia Mecânica, Departamento de Engenharia Mecânica, Universidade Estadual de Maringá – UEM, Maringá, PR, Brasil
[2]Laboratório de Química, Departamento de Química, Universidade Estadual de Maringá – UEM, Maringá, PR, Brasil
[3]Laboratório de Bioprocessos e Biotecnologia, Coordenação de Engenharia de Bioprocessos e Biotecnologia, Universidade Tecnológica Federal do Paraná – UTFPR, Dois Vizinhos, PR, Brasil

*gabriel_fornazaro@hotmail.com

Abstract

Composites of polyamide 6.6 (PA 6.6) reinforced with glass fibers exhibit strong mechanical properties; however, the hygroscopic nature of PA 6.6 introduces variability due to water absorption, which can affect these properties. This study aimed to develop a statistical model to assess the impact of hydration on the mechanical properties of PA 6.6/glass fiber composites. A 2^3 factorial design was employed to analyze the effects of time, temperature, and glass fiber content on tensile strength, impact resistance, and flexural properties. Characterization of the composites using scanning electron microscopy (SEM), X-ray diffraction (XRD), and differential scanning calorimetry (DSC) revealed excellent fiber-matrix adhesion and an increased degree of crystallinity, which contributed to enhanced Young's modulus. The analysis showed that time and temperature were the primary factors influencing water absorption. A statistical model was created to predict the mechanical properties of the composites, incorporating the effects of hydration directly into the predictions.

Keywords: *hydration, mechanical properties, PA 6.6, optimization.*

1. Introduction

Polyamide 6.6 (PA 6.6) is a widely utilized engineering plastic known for its high performance and technical reliability in manufacturing various parts[1,2]. Its long-standing success and reliability over more than five decades make it one of the most established materials in the industry[2,3]. However, despite its widespread use, PA 6.6 presents significant challenges related to moisture absorption, which can negatively impact its mechanical properties, particularly in environments with fluctuating humidity. Understanding these effects is critical for industries, such as automotive and electronics, where material performance under different environmental conditions is essential. PA 6.6 is produced through polycondensation reactions between adipic acid and hexamethylenediamine. The planar zigzag structure of the PA chains facilitates intermolecular hydrogen bonding, resulting in a strong, dense, and crystalline polymer[3]. The degree of crystallinity, which is directly related to the spacing of the hydrogen bonds, can be influenced by adsorbed moisture[4,5], significantly affecting the mechanical properties of PA 6.6 and making it more ductile[2,6].

The chemical properties of PA 6.6 allow for the incorporation of various additives, including elastomers, mineral fillers, and glass fibers (GF), among others[5,7-9]. These additions enhance its properties, enabling PA 6.6 to replace metals, thermosets, and other construction materials. Glass fibers are the most used reinforcing agents in PA 6.6 composites[7,10-12], due to their favorable chemical and physical characteristics, such as a high strength-to-weight ratio, resistance to high temperatures, and resistance to corrosion and moisture[1,8]. Glass fiber-reinforced PA 6.6 composites are extensively employed in the automotive industry, agricultural parts, and electrical components, with commercial composites typically containing 10 to 30 wt% GF. The high tensile strength of glass fibers enhances the composite's resistance, increasing both Young's modulus and flexural modulus, as well as tensile strength. Conversely, the hygroscopic nature of the polymer matrix tends to increase ductility and reduce tensile strength[12-14]. However, the interaction between glass fibers and the PA 6.6 matrix is significantly affected by water absorption, which compromises the material's mechanical integrity over time.

Previous studies have demonstrated the adverse effects of water absorption on the mechanical performance of PA 6.6/glass fiber composites, but there is limited information on the behavior of these materials under controlled hydration conditions, such as partial saturation at different humidity levels. Research has shown that water absorption adversely affects the mechanical properties of PA 6.6/glass fiber composites. Chaichanawong et al.[13] investigated the impact of moisture absorption on these properties by immersing composites in distilled water for 60 days, noting significant changes in mechanical performance, including peak load impact responses across various energy levels. Zhang et al.[15] focused on the diffusion coefficient and final moisture concentration in composites subjected to different hydration conditions. Their findings indicated that equilibrium moisture concentration was influenced by relative humidity and fiber content, with moisture diffusion effects varying according to humidity-temperature interactions. Hassan et al.[16] reported that specimens in wet conditions exhibited lower tensile strength and modulus compared to dry composites, while fracture strain increased under approximately 50% relative humidity. Despite the extensive data provided by polymer and composite suppliers for dried materials, information under other conditions, such as saturation at 50% relative humidity, is often scarce. In the plastic injection and processing industry, it is crucial to understand the mechanical properties of materials under conditions not covered in standard data sheets, especially for parts with tight assembly tolerances.

This gap in knowledge is particularly relevant for manufacturing industries where precise mechanical performance is crucial, especially for components that must meet tight assembly tolerances. This study aims to assess the impact of hydration time and temperature on the mechanical properties of PA 6.6 composites with 10 to 30 wt% glass fiber, reflecting common commercial compositions. A statistical model was developed to predict the tensile strength and impact resistance of these composites under the studied conditions. Additionally, to minimize the thermal energy required in industrial hydration processes, temperatures below 40 °C were investigated, with a view to utilizing water from cooling processes of injection molds or leveraging solar energy.

2. Materials and Methods

2.1 Materials and specimens processing

Polyamide 6.6 in its pure form and with various glass fiber contents were sourced from Petropol Polímeros® and processed by Haplos Indústria e Comércio Ltda. The materials studied included: Polyamide 6.6 (Nypol A3 HL NR310), Polyamide with 10% Glass Fiber (Nypol A3 G10 NR512), Polyamide with 20% Glass Fiber (Nypol G20 NR441), and Polyamide with 30% Glass Fiber (Nypol G30 NR399). The raw material was provided in pellet form and without pigmentation; it was dried in an oven at 90 °C for 4 hours.

To prepare the specimens, composites of the PA 6.6 matrix reinforced with glass fiber (PA/GF) were produced with 10, 20, and 30 wt% glass fiber content (denoted as PA/GF10, PA/GF20, and PA/GF30, respectively). The injection molding of the specimens, adhering to ASTM D638-2a Type

I and ASTM D256 standards, was performed using an MG 100/200 injection machine. The process parameters included a barrel temperature of 275 °C, mold temperature of 80 °C, injection pressure of 90 bar, holding pressure of 40 bar, and an injection speed of 80 mm/s. The specimens were then stored in an airtight package until they were subjected to hydration. Six specimens per condition were prepared to ensure accurate measurement and minimize errors.

2.2 Design of experiments

A full factorial design (Montgomery, 2013) was implemented as a statistical method for all mechanical testing after the hydration to evaluate the main factors and to develop mathematical models to predict PA/GF mechanical properties. The factors were glass fiber percentage (X_1), hydration temperature (X_2) and hydration time (X_3), as shown in Table 1. The responses were named as the moisture absorption (Y_1), young's modulus (Y_2), yield strength (Y_3), strain (Y_4) and impact strength (Y_5). The inputs and responses were drawn up in a 2^3 full factorial design with 8 base runs, 4 central points and a replicate, to generate 20 total runs to each response, providing the optimized conditions for the hydration related to the yield and the mechanical responses. R Studio 3.5.0 software was used for statistics at 0.05 level of significance.

The analysis of variance (ANOVA) was used as statistical method to analyze the effect of glass fiber and hydration on the mechanical response of the composites. These ANOVA tests allow us to generate a mathematical model as shown by follow statistical model (Equation 1):

$$y = \beta_0 + \sum_{i=1}^{k}\beta_i X_i \sum_{i=1}^{k}\beta_{ii} X_i^2 + \sum_{i=1}^{k}\sum_{j=1}^{k}\beta_{ij} X_i X_j + \in \qquad (1)$$

where X_i and X_j are the independent input variables where the response y depends on them and the experimental errors term, denoted as $\in$. The y will be proposed using the second order polynomial regression model, which is called the quadratic model. The β_i represents the linear effect of X_i, β_{ii} represents the quadratic effect of X_i^2 and β_{ij} reveals the linear-by-linear interaction between X_i and X_j.

2.3 Moisture absorption

The hydration was performed in a thermostatic bath, Tecnal TE-184, using deionized water. The weights of specimens were measured in an analytical balance (Denver Instruments APX-200 with a resolution of 0.1 mg) before and after the treatment. Equation 2 was used to calculate the amount of absorbed water.

$$A_{ab} = \frac{m_h - m_i}{m_i} * 100 \qquad (2)$$

where m_i and m_h are the weight of samples in the beginning and after hydration, respectively.

2.4 Tensile strength test

The tensile strength tests were performed according to ASTM D638 in a universal testing machine, EMIC DL

Table 1. Experimental factors, their levels, and responses for 2^3 full factorial design with four central points.

Run	Factors			Responses				
	X_1	X_2	X_3	Y_1	Y_2	Y_3	Y_4	Y_5
	Glass Fiber (%)	Temperature (°C)	Time (days)	Moisture absorption (%)	Young's Modulus (MPa)	Yield Strength (MPa)	Strain (%)	Impact strength (J/m)
1	(-1)10	(-1) 25.0	(+1) 8.0	2.78500	1130.9	30.16	3.13	99.03
2	(-1) 10	(-1) 25.0	(-1) 1.0	1.08200	1260.7	35.22	5.64	48.38
3	(-1) 10	(+1) 40.0	(-1) 1.0	1.64877	974.8	43.56	4.76	69.87
4	(-1) 10	(+1) 40.0	(+1) 8.0	4.45257	669.3	43.36	13.81	202.72
5	(+1) 30	(-1) 25.0	(-1) 1.0	0.84120	2423.9	122.19	7.41	138.82
6	(+1) 30	(+1) 40.0	(-1) 1.0	1.86349	1243.2	103.85	9.04	224.43
7	(+1) 30	(+1) 40.0	(+1) 8.0	3.55114	1292.8	89.79	10.58	321.17
8	(+1) 30	(-1) 25.0	(+1) 8.0	2.12500	2143.3	107.29	7.60	212.46
9	(+1) 30	(+1) 40.0	(+1) 8.0	3.48092	1247.8	74.10	10.58	331.37
10	(-1) 10	(-1) 25.0	(-1) 1.0	1.09415	1260.7	37.82	3.16	52.22
11	(0) 20	(0) 32.5	(0) 4.5	2.26312	1534.2	59.90	7.84	186.25
12	(0) 20	(0) 32.5	(0) 4.5	2.15641	1544.4	62.03	8.07	180.48
13	(+1) 30	(-1) 25.0	(+1) 8.0	2.11762	2210.5	80.00	5.75	175.67
14	(+1) 30	(+1) 40.0	(-1) 1.0	1.24532	1799.0	88.47	6.63	151.90
15	(-1) 10	(+1) 40.0	(+1) 8.0	4.48164	658.4	43.88	15.55	280.18
16	(0) 20	(0) 32.5	(0) 4.5	2.17544	1643.6	60.30	7.37	191.51
17	(-1) 10	(-1) 25.0	(+1) 8.0	2.77466	1255.7	29.28	3.16	119.73
18	(+1) 30	(-1) 25.0	(-1) 1.0	0.85181	2020.0	93.89	5.54	127.35
19	(0) 20	(0) 32.5	(0) 4.5	2.20392	1594.0	61.12	8.30	193.37
20	(-1) 10	(+1) 40.0	(-1) 1.0	1.58727	1210.6	34.64	3.14	73.77

10000, using a load cell of 20 kN under 5 mm/min speedup to the failure. The results of all mechanical properties are averages of five tested specimens.

2.5 Izod impact test

The impact resistance tests were carried out in the CEAST equipment with pendulum 2.75 J, model Resil Impactor Junior, according to ASTM D256.The notch specimens were prepared using a CEAST Notchvis machine with a resolution of 1 μm. The results of all mechanical properties are averages of five tested specimens.

2.6 Scanning electron microscopy (SEM)

Scanning electron microscopy images of the fractured specimens from tensile tests, previously coated with gold by sputtering, were taken using a QUANTA 250 equipment from FEI, with a magnification of 250x.

2.7 X-ray diffraction analysis (XRD)

X-ray diffraction analysis was performed at room temperature on a Shimadzu X-ray diffractometer, model XRD-7000, with Cu-Kα radiation(λ = 1.5406 Å) in a current of 30 mA, and potential of 40 kV at 2°/min from 10 to 40° (2θ).

2.8 Differential scanning calorimetry (DSC)

DSC analyses were carried out on DSC-Q20 (TA instruments), using no hermitic aluminum pans, heating and cooling rates of 10 °C/min, from 25 to 300 °C, under

compressed air flux of 50 mL/min. Equation 3 was used to determine the degree of crystallinity of the polymer matrix.

$$X = \frac{\Delta H_f}{\Delta H_f{}^\circ}100 \tag{3}$$

where ΔH_f is the heat of fusion of the sample and $\Delta H_f{}^\circ$ is the heat of fusion of a hypothetically 100% crystalline polymer. In the case of PA 6.6 the value of $\Delta H_f{}^\circ$ used was 195 J/g, frequently mentioned in the literature[14,17].

3. Results and Discussions

3.1 Statistical analysis

Five primary experiments were conducted for all mechanical tests, with the results of the tensile testing presented in Figure 1. The factorial experimental design was employed as the statistical methodology to analyze the impact of water absorption on various mechanical properties, considering the influence of factors such as glass fiber content, temperature, and treatment duration. The experimental factors, their respective levels, and the observed responses are detailed in Table 1.

The statistical analysis was conducted at a significance level of 0.05, utilizing R Studio 3.5.0 software to calculate the effects of various model terms through regression analysis. The p-values obtained indicated that all factors and their interactions significantly affected the moisture absorption response (Y1), with a p-value of less than 0.05.
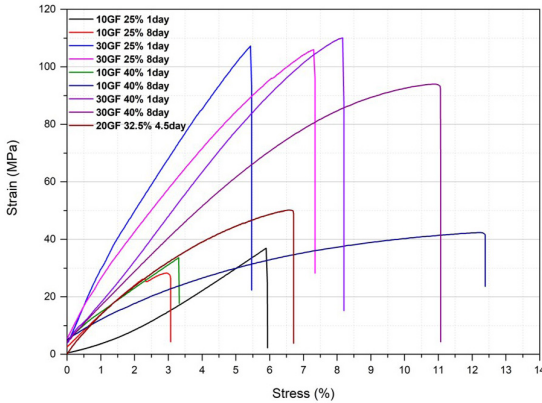
Figure 1. The tensile mechanical test data.

The mathematical model describing the factors influencing moisture absorption is given by:

$$Moisture\ absorption\ (Y1) = 2.239073 - 0.23935X_1 + 0.53998X_2 + 0.97216X_3 - 0.16305X_1 : X_3 + 0.23052X_2 : X_3$$

$$R^2 = 98.81\%.$$

For other responses, the mathematical models are as follows:

$$Young's\ modulus\ (Y2) = 1488.9 + 372.5X_1 - 288.1X_2 - 99.0X_3 - 113.7X_1 : X_2$$

$$R^2 = 91.79\%.$$

$$Yield\ Strength\ (Y3) = 50.00 + 19.86X_1 - 9.13X_3$$

$$R^2 = 83.01\%.$$

$$Strain\ (Y4) = 7.35 + 0.67X_1 + 2.05X2 + 1.55X3 - 0.7267X1 : X2 - 0.82X1 : X3 + 1.82X2 : X3 - 1.18X1 : X2 : X3$$

$$R^2 = 93.58\%.$$

$$Impact\ Strength\ (Y5) = 169.03 + 46.1X_1 + 42.6X2 + 53.5X3 + 23.5X2 : X3$$

$$R^2 = 93.28\%.$$

The analysis of variance (ANOVA) confirmed the goodness of fit for the mathematical models, with R-squared values of 0.988 for moisture absorption, 0.9179 for Young's modulus, 0.8301 for yield strength, 0.9358 for strain, and 0.9328 for impact strength. The F-Test values (p-values) were less than 0.05, indicating that the null hypothesis could be rejected with a probability of less than 5%. Therefore, the models obtained were deemed significant, as the p-values were substantially smaller than 0.05, and the R-squared values were close to 1.0, demonstrating a good fit to the experimental data.

To validate and verify the accuracy of the models, a software tool for easy industry verification was developed,

and the results showed good correlation with the experimental findings. These results will be detailed in a future publication. The mathematical models indicated excellent correspondence with the experimental data.

The ANOVA analysis identified statistically significant interactions. Time (X3) had the greatest effect on moisture absorption (Y1), with minimal impact on Young's modulus. Glass fiber content (X1) significantly influenced Young's modulus, and similar trends were observed for yield strength (Y3), where X1 and X3 were the major factors. Temperature (X2) had the most substantial effect on strain (Y4), while X3 had the most significant influence on impact strength (Y5).

According to ANOVA, all main effects and some interaction effects were statistically significant for moisture absorption (Y1), except for the interactions X1X2 (glass fiber and temperature) and X1:X2:X3 (glass fiber, temperature, and time), which had p-values greater than 0.05, rendering them statistically insignificant. Hydration time (X3) and temperature (X2) were the primary factors influencing moisture absorption, with time being more critical. The presence of glass fiber limited moisture absorption, as it does not absorb water as significantly as natural fibers[15,18]. For Young's modulus (Y2), ANOVA revealed that all main effects and the X1X2 interaction were statistically significant. The amount of glass fiber (X1) had the most substantial effect on Young's modulus, followed by temperature (X2). Increased fiber content required greater force to achieve deformation, enhancing the material's resistance to tensile stresses. In contrast, higher hydration temperatures reduced Young's modulus by improving treatment efficiency and increasing the material's ductility[15,19-22].

Yield strength (Y3) was primarily influenced by glass fiber content (X1) and time (X3), with the former having the most significant impact. Increased glass fiber content improved tensile strength, while hydration time affected the efficiency of the hydration process, impacting the material's ductility and yield point[13].

For strain (Y4), all inputs were statistically significant, with temperature (X2), time (X3), and their interaction (X2X3) being the primary contributors. Increased temperature and hydration time improved the composite's ductility, as evidenced by stress-strain curves f other studies[23,24]. The relationship between Young's modulus and strain was well-documented, with hydration leading to increased strain due to plasticization of the polymer matrix[13].

Impact strength (Y5) showed that all main effects were statistically significant, with the X2X3 interaction also significant. Glass fiber content (X1), temperature (X2), and time (X3) contributed significantly to impact resistance, with each factor positively influencing the response. The increase in temperature and time improved the material's ductility, enhancing its energy dissipation upon impact. Although higher glass fiber content increased material fragility, the fibers helped prevent crack propagation, consistent with findings by Yoo et al.[25] and Hancox and Wells[26].

To optimize the responses of glass fiber content (X1), temperature (X2), and time (X3) on moisture absorption, Young's modulus, yield strength, strain, and impact strength,

response surface methodology was employed. Three-dimensional plots generated from this analysis are shown in Figure 2. Figure 2a illustrates that moisture absorption increased with temperature (X2) and time (X3), while glass fiber content (X1) had a minimal effect. For Young's modulus (Y2), increased glass fiber content (X1) improved the response, as shown in Figure 2b. Yield strength (Y3), depicted in Figure 2c, was most affected by glass fiber content (X1), with minimal influence from temperature (X2) and time (X3). Strain (Y4) increased with temperature (X2) and time (X3), as shown in Figure 2d, while impact strength (Y5) increased with all factors, as demonstrated in Figure 2e.

Increasing the fiber content in polyamide 6.6 (PA 6.6) composites leads to increased fragility, accompanied by higher values of Young's modulus, yield strength, and strain, which are intrinsically proportional. The incorporation of glass fibers into the PA 6.6 matrix results in composites that absorb less energy and exhibit a lower damping factor compared to the pure polymer. The absorption of moisture in the composites is directly proportional to both the temperature and duration of hydration, leading to a reduction in the material's crystalline regions and glass transition temperature. This effect occurs because water acts as a plasticizer, thereby affecting the composite's mechanical properties.

Under the conditions examined, the impact of hydration was most pronounced on Young's modulus and strain. The glass fiber content significantly influenced yield strength, aligning with findings by Chaichanawong[13]. However, increased temperature and hydration time were responsible for enhancing the material's ductility, allowing it to dissipate more energy upon impact. In addition to the response surface plots, the adequacy and predictive capability of the developed model, as verified by the software created by the authors, are detailed in Table 2.

3.2 SEM

The SEM images of the fracture surfaces from the tensile test specimens, shown in Figure 3, reveal distinct fracture characteristics under varying hydration conditions. Specifically, ductile fractures are evident in specimens that experienced higher water absorption. Notably, samples hydrated at 25 °C for 1 day exhibit a higher prevalence of fragile fractures, characterized by a greater number of fiber pull-outs. In contrast, specimens treated at 40 °C for 8 days display regions with ductile fractures. The SEM analysis indicates good interfacial adhesion between the fibers and the matrix. However, as hydration temperature and duration increase, the presence of crevice lines between the fiber and matrix becomes more apparent, which adversely affects the mechanical properties. Additionally, the SEM images reveal fiber-matrix adhesion, which contributes to a significant increase in Young's modulus and yield strength. This increase is attributed to the high variability in the cross-section of the fibers within the matrix, particularly in composites with higher fiber content[13,14,25].

3.3 XRD

The X-ray diffraction patterns, depicted in Figure 4, reveal two prominent peaks indicative of the presence of the α phase in polyamide 6.6 (PA 6.6). The first peak at $2\theta = 20.2°$ corresponds to the distances between chains connected by hydrogen bonds in the plane (100), while the second peak at $2\theta = 22.6°$ relates to the planes (010) and (110), representing the separation between layers bound by hydrogen bonds[17,26-28]. It is noteworthy that the peak thickness was consistent across all samples.

An observed decrease in peak resolution and an increase in the amorphous halo with higher glass fiber content indicate a reduction in the degree of crystallinity of the composite. This reduction is attributed to the physical obstruction created by the fibers within the matrix, which impedes polymer packing and increases the average distance between the chains, as previously noted by Ota et al.[27].

3.4 DSC

The melting temperature of the PA 6.6 matrix was approximately 260 °C, as shown in Figure 5. This value aligns with previously reported data[14,29] and is consistent with the information provided in the supplier's data sheet. Additionally, a notable curvature in the region around 100 °C indicates the presence of adsorbed water within the samples[30,31].

Table 3 displays the values for the heat of fusion and the calculated degree of crystallinity (DC) of the composites, as determined using Equation 2. The degree of crystallinity was found to decrease with increasing temperature and hydration time, which aligns with the observations from the X-ray diffraction (XRD) analysis. According to Fabre et al.[32,33], an increase in the degree of crystallinity typically leads to higher Young's modulus and yield stress. In this study, higher values of Young's modulus and yield stress were observed in samples with the same fiber content but hydrated for shorter times and at lower temperatures, which resulted in lower degrees of crystallinity. These findings are consistent with the results obtained from both the XRD and differential scanning calorimetry (DSC) analyses.

Table 2. Comparison between the model and the results obtained for the test condition to 10% at 36 °C for 3 days.

| Properties	model	Exp. results
Moisture absorption (%)	2.20 ± 0.13	2.57 ± 1.87
Young's Modulus (MPa)	1042.53 ± 162.91	1351.00 ± 65.28
Yield Strength (MPa)	34.51 ± 5.19	33.68 ± 11.02
Strain (%)	6.22 ± 0.91	5.87 ± 1.49
Impact strength (J/m)	106.13 ± 25.99	76.91 ± 5.6

Table 3. Thermal characteristic and degree of crystallinity of PA6.6/GF composites hydrated under boundary conditions.

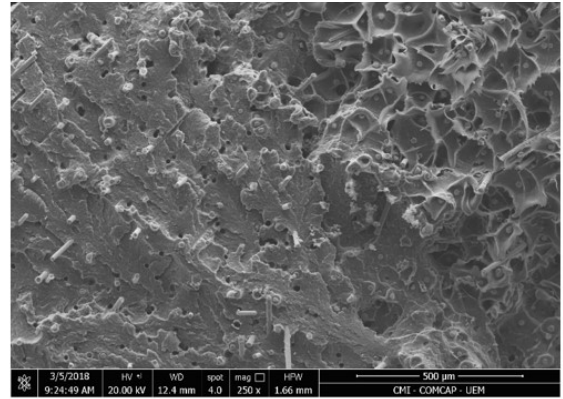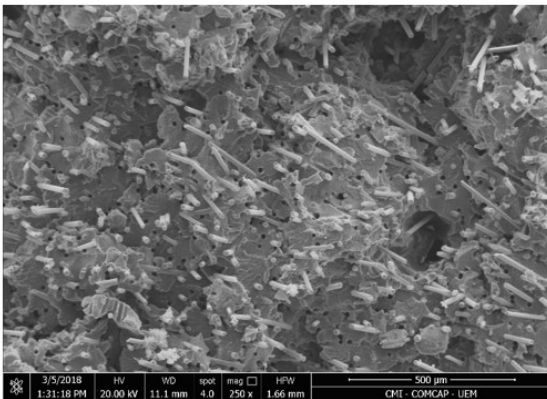| Glass fiber (%)	Temperature (°C)	Time (days)	DC (%)
10	25	1	20.20
10	40	8	17.81
30	25	1	19.27
30	40	8	16.31

DC = degree of crystallinity.
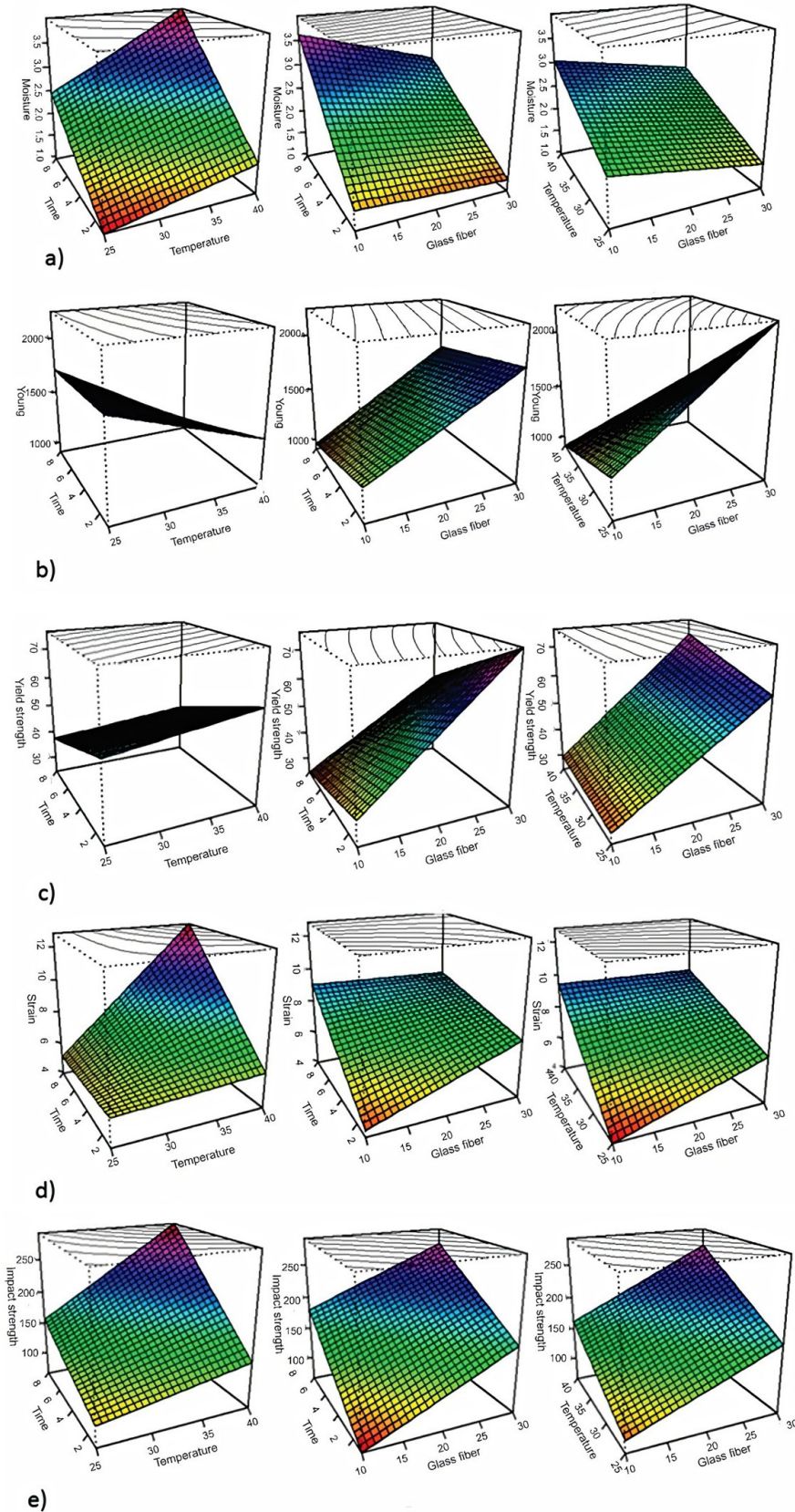
Figure 2. Response surface plots showing the effects X1 (glass fiber), X2 (Temperature) and X3 (Time) on the moisture absorption (a), Young's modulus (b), yield strength (c), strain (d) and impact strength (e).
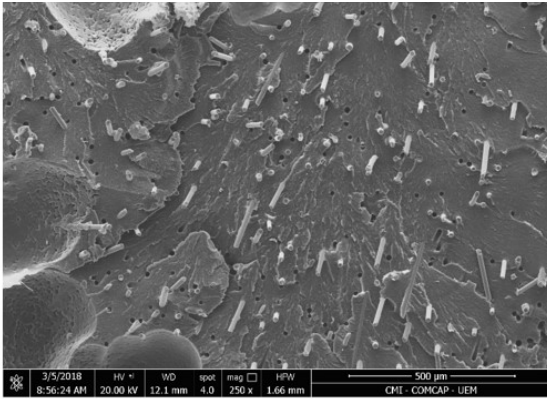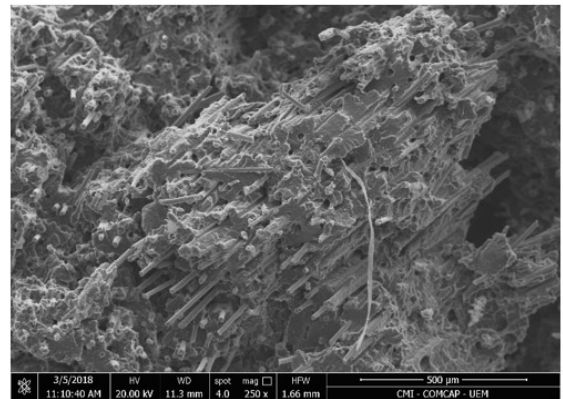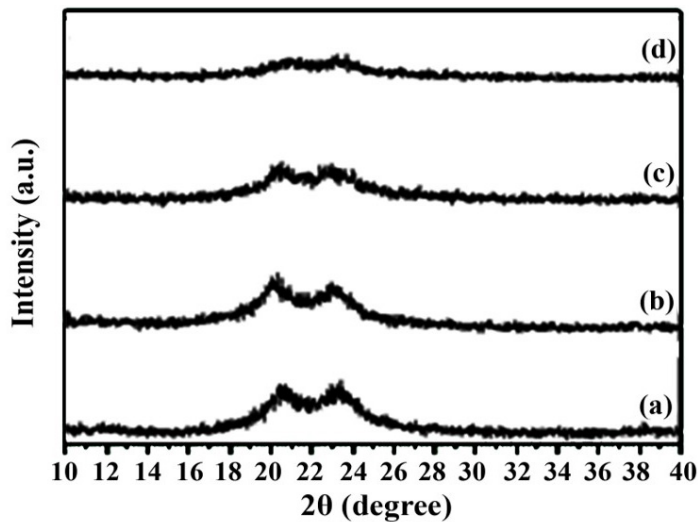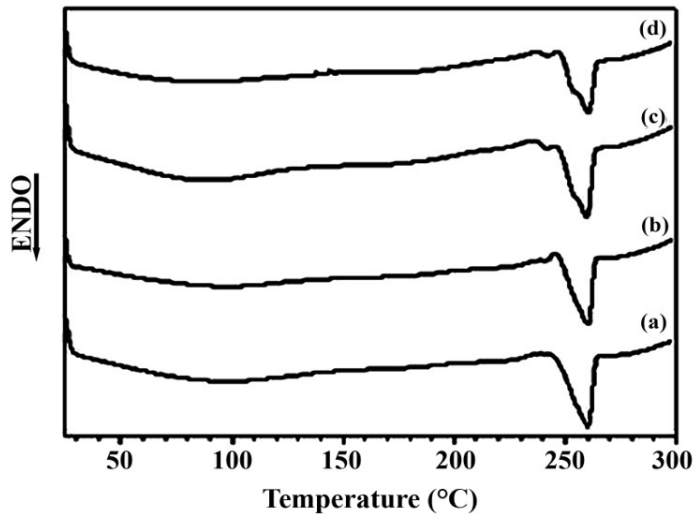
Figure 3. SEM images of PA6.6/GF composites hydrated under boundary conditions (a) 10% GF 25 °C 1 day, (b) 10% GF 40 °C 8 days, (c) 30% GF 25 °C 1 day and (d) 30% GF 40 °C 8 days.

Figure 4. X-ray Patterns of PA6.6/GF composites hydrated under boundary conditions (a) 10% GF 25 °C 1 day, (b) 10% GF 40 °C 8 days, (c) 30% GF 25 °C 1 day and (d) 30% GF 40 °C 8 days.

Figure 5. DSC curves of PA6.6/GF composites hydrated under boundary conditions (a) 10% GF 25 °C 1 day, (b) 10% GF 40 °C 8 days, (c) 30% GF 25 °C 1 day and (d) 30% GF 40 °C 8 days.

4. Conclusions

The conclusion addresses the study objectives by detailing how the influence of hydration parameters and fiber reinforcement on the mechanical properties of polyamide 6.6 (PA 6.6) composites with glass fibers was thoroughly investigated. The influence of hydration parameters and fiber reinforcement on the mechanical properties of polyamide 6.6 (PA 6.6) composites with glass fibers was thoroughly qualified and quantified through mechanical testing and statistical analysis. The primary factors affecting the amount of water absorbed by the composites were found to be hydration time and temperature, in that order of significance. The glass fiber content emerged as the most influential parameter on the mechanical properties of the composites, positively affecting all properties except for strain, confirming the study's aim to assess how fiber reinforcement affects these properties. The presence of glass fibers also impeded crack propagation during rupture and led to a reduction in the degree of crystallinity of the PA 6.6 matrix. The mechanical test results were corroborated by characterization techniques, fulfilling the objective of validating the findings.

Furthermore, the development of a statistical model to predict tensile strength, impact strength, and flexural properties directly supports the study's objective of providing predictive capabilities under various conditions. A statistical model was developed to predict the tensile strength, impact strength, and flexural properties of the composites under the studied conditions. To facilitate the application and understanding of these statistical models, a software tool named HIDRAPA was created. This tool aims to simplify and enhance access to the predictive capabilities of the model.

5. Author's Contribution

• **Conceptualization** – Silvia Luciana Favaro.

• **Data curation** – Allan Oliveira Rodrigues.

• **Formal analysis** – Andressa dos Santos.

• **Funding acquisition** - Eduardo Radovanovic; Silvia Luciana Favaro.

• **Investigation** – Allan Oliveira Rodrigues.

• **Methodology** – Allan Oliveira Rodrigues.

• **Project administration** – Silvia Luciana Favaro.

• **Resources** – Silvia Luciana Favaro.

• **Software** – NA.

• **Supervision** – Silvia Luciana Favaro.

• **Validation** – Eduardo Radovanovic.

• **Visualization** – Gabriel Fornazaro; Gabriel Vinicius Alves Silva.

• **Writing – original draft –** Antonio Guilherme Basso Pereira.

• **Writing – review & editing** – Antonio Guilherme Basso Pereira; Gabriel Fornazaro; Gabriel Vinicius Alves Silva; Andressa dos Santos; Hederson Majela do Nascimento.

6. Acknowledgements

7. References

1. Wiebeck, H., & Harada, J. (2005). *Plásticos de engenharia: tecnologia e aplicações*. São Paulo: Editora Artilber.

2. Djukic, S., Bocahut, A., Bikard, J., & Long, D. R. (2020). Mechanical properties of amorphous and semi-crystalline semi-aromatic polyamides. *Heliyon*, 6(4), e03857. http://doi.org/10.1016/j.heliyon.2020.e03857. PMid:32368659.

3. Simielli, E. R., & Santos, P. A. (2010). *Plásticos de engenharia: principais tipos e sua moldagem por injeção*. São Paulo: Artilber.

4. Sun, J., Zhang, D., Yang, Y., Guo, Z., Fang, Z., Chen, P., & Li, J. (2023). Improving flame retardancy and mechanical properties of polyamide 6 induced by multiple reactions among flame retardants and matrix. *Reactive & Functional Polymers*, *187*, 105590. http://doi.org/10.1016/j.reactfunctpolym.2023.105590.

5. Wang, Q., Ge, M., Dou, Y., Yang, F., Wang, J., Shao, Y., & Huang, A. (2020). Engineering ultrafine Pd clusters on laminar polyamide: a promising catalyst for benzyl alcohol oxidation under air in water. *Molecular Catalysis*, *497*, 111203. http://doi.org/10.1016/j.mcat.2020.111203.

6. Arif, M. F., Meraghni, F., Chemisky, Y., Despringre, N., & Robert, G. (2014). In situ damage mechanisms investigation of PA66/GF30 composite: effect of relative humidity. *Composites. Part B, Engineering*, *58*, 487-495. http://doi.org/10.1016/j.compositesb.2013.11.001.

7. Callister, W. D., Jr., & Rethwisch, D. G. (2016). *Ciência e engenharia de materiais: uma introdução*. Rio de Janeiro: LTC.

8. McIntee, O. M., Welch, B. C., Greenberg, A. R., George, S. M., & Bright, V. M. (2022). Elastic modulus of polyamide thin films formed by molecular layer deposition. *Polymer*, *255*, 125167. http://doi.org/10.1016/j.polymer.2022.125167.

9. Fajardo-Diaz, J. L., Takeuchi, K., Morelos-Gomez, A., Cruz-Silva, R., Yamanaka, A., Tejima, S., Izu, K., Saito, S., Ito, I., Maeda, J., & Endo, M. (2023). Enhancing boron rejection in low-pressure reverse osmosis systems using a cellulose fiber–carbon nanotube nanocomposite polyamide membrane: a study on chemical structure and surface morphology. *Journal of Membrane Science*, *679*, 121691. http://doi.org/10.1016/j.memsci.2023.121691.

10. Fu, X., Wang, J., He, Y., Ji, Y., Bi, Q., Wang, X., & Liu, F. (2023). Nanofiltration membrane with asymmetric polyamide dual-layer through interfacial polymerization for enhanced separation performance. *Desalination*, *564*, 116806. http://doi.org/10.1016/j.desal.2023.116806.

11. Sam-Daliri, O., Ghabezi, P., Steinbach, J., Flanagan, T., Finnegan, W., Mitchell, S., & Harrison, N. (2023). Experimental study on mechanical properties of material extrusion additive manufactured parts from recycled glass fibre-reinforced polypropylene composite. *Composites Science and Technology*, *241*, 110125. http://doi.org/10.1016/j.compscitech.2023.110125.

12. Petrașcu, O.-L., & Pascu, A.-M. (2023). Comparative study of polyamide 6 (PA6) and polyamide 6 reinforced with 30% of glass fiber (PA6GF30). *Materials Today: Proceedings*, *6*(Part 4), 625-626. http://doi.org/10.1016/j.matpr.2023.04.112.

13. Chaichanawong, J., Thongchuea, C., & Areerat, S. (2016). Effect of moisture on the mechanical properties of glass fiber reinforced polyamide composites. *Advanced Powder Technology*, *27*(3), 898-902. http://doi.org/10.1016/j.apt.2016.02.006.

14. Ştefănoaea, N., & Pascu, A. M. (2022). Study of implementation the tensile data of the glass fiber reinforced polyamide into the finite element analyses. *Materials Today: Proceedings*, *93*(Part 4), 736-742. http://doi.org/10.1016/j.matpr.2023.06.026.

15. Zhang, S., Huang, Z., Zhang, Y., & Zhou, H. (2015). Experimental investigation of moisture diffusion in short-glass-fiber-reinforced polyamide 6,6. *Journal of Applied Polymer Science*, *132*(37), 42369. http://doi.org/10.1002/app.42369.

16. Hassan, A., Rahman, N. A., & Yahya, R. (2012). Moisture absorption effect on thermal, dynamic mechanical and mechanical properties of injection-molded short glass-fiber/polyamide 6, 6 composites. *Fibers and Polymers*, *13*(7), 899-906. http://doi.org/10.1007/s12221-012-0899-9.

17. Teixeira, D., Giovanela, M., Gonella, L. B., & Crespo, J. S. (2013). Influence of flow restriction on the microstructure and mechanical properties of long glass fiber-reinforced polyamide 6.6 composites for automotive applications. *Materials & Design*, *47*, 287-294. http://doi.org/10.1016/j.matdes.2012.12.030.

18. Montgomery, D. C. (2013). *Design and analysis of experiments*. New York: John Wiley & Sons.

19. Kumar Maurya, A., Kumar, S., Singh, M., & Manik, G. (2023). Polyamide fiber reinforced polymeric composites: a short review. *Materials Today: Proceedings*, *80*(Part 1), 98-103. http://doi.org/10.1016/j.matpr.2022.10.171.

20. Pai, R., Bangarappa, L., Lokesh, K. S., Shrinivasa Mayya, D., Naveen, C. R., & Pinto, T. (2022). Hybridization effect on water absorption and flexural properties of E-glass/banana fibre/epoxy composites. *Materials Today: Proceedings*, *52*(Part 3), 1841-1845. http://doi.org/10.1016/j.matpr.2021.11.491.

21. Silva, L., Tognana, S., & Salgueiro, W. (2013). Study of the water absorption and its influence on the Young's modulus in a commercial polyamide. *Polymer Testing*, *32*(1), 158-164. http://doi.org/10.1016/j.polymertesting.2012.10.003.

22. Pizzorni, M., & Prato, M. (2023). Effects of hygrothermal aging on the tensile and bonding performance of consolidated 3D printed polyamide-6 composites reinforced with short and multidirectional continuous carbon fibers. *Composites. Part A, Applied Science and Manufacturing*, *165*, 107334. http://doi.org/10.1016/j.compositesa.2022.107334.

23. Taktak, R., Guermazi, N., Derbeli, J., & Haddar, N. (2015). Effect of hygrothermal aging on the mechanical properties and ductile fracture of polyamide 6 : experimental and numerical approaches. *Engineering Fracture Mechanics*, *148*, 122-133. http://doi.org/10.1016/j.engfracmech.2015.09.001.

24. Ferreño, D., Carrascal, I., Ruiz, E., & Casado, J. A. (2011). Characterisation by means of a finite element model of the influence of moisture content on the mechanical and fracture properties of the polyamide 6 reinforced with short glass fibre. *Polymer Testing*, *30*(4), 420-428. http://doi.org/10.1016/j.polymertesting.2011.03.001.

25. Yoo, Y., Spencer, M. W., & Paul, D. R. (2011). Morphology and mechanical properties of glass fiber reinforced Nylon 6 nanocomposites. *Polymer*, *52*(1), 180-190. http://doi.org/10.1016/j.polymer.2010.10.059.

26. Hancox, N. L., & Wells, H. (1973). Izod impact properties of carbon-fibre/glass-fibre sandwich structures. *Composites*, *4*(1), 26-30. http://doi.org/10.1016/0010-4361(73)90292-9.

27. Ota, W. N., Amico, S. C., & Satyanarayana, K. G. (2005). Studies on the combined effect of injection temperature and fiber content on the properties of polypropylene-glass fiber composites. *Composites Science and Technology*, *65*(6), 873-881. http://doi.org/10.1016/j.compscitech.2004.10.025.

28. Li, J., Zuo, Y., Cheng, X., Yang, W., Wang, H., & Li, Y. (2009). Preparation and characterization of nano-hydroxyapatite/polyamide 66 composite GBR membrane with asymmetric porous structure. *Journal of Materials Science. Materials in Medicine*, *20*(5), 1031-1038. http://doi.org/10.1007/s10856-008-3664-2. PMid:19115093.

29. Ji, W., Wang, X., Ding, T., Chakir, S., Xu, Y., Huang, X., & Wang, H. (2023). Electrospinning preparation of nylon-6@UiO-66-NH2 fiber membrane for selective adsorption enhanced photocatalysis reduction of Cr(VI) in water. *Chemical Engineering Journal*, *451*(Part 4), 138973. http://doi.org/10.1016/j.cej.2022.138973.

30. Wang, K., Zhao, K., Meng, Q., Li, X., Bai, Q., Jiao, H., & Tang, Y. (2022). Preparation of zirconium carbide nanofibers by electrospinning of pure zirconium-containing polymer. *Ceramics International*, *48*(17), 25474-25483. http://doi.org/10.1016/j.ceramint.2022.05.226.

31. Wang, P., Ke, L., Sze, A. N. S., Wang, Z., Zhao, J., Li, W., & Leung, C. K. Y. (2023). Effects of relative humidity, alkaline concentration and temperature on the degradation of plain/

coated glass fibers: experimental investigation and empirical degradation model. *Construction & Building Materials*, *391*, 131757. http://doi.org/10.1016/j.conbuildmat.2023.131757.

32. Men, Y., & Rieger, J. (2004). Temperature dependent wide angle X-ray diffraction studies on the crystalline transition in water saturated and dry polyamide 6/66 copolymer. *European Polymer Journal*, *40*(11), 2629-2635. http://doi.org/10.1016/j.eurpolymj.2004.07.003.

33. Fabre, V., Quandalle, G., Billon, N., & Cantournet, S. (2018). Time-temperature-water content equivalence on dynamic mechanical response of polyamide 6, 6. *Polymer*, *137*, 22-29. http://doi.org/10.1016/j.polymer.2017.10.067.